Solar Phys (2020) 295:164
https://doi.org/10.1007/s11207-020-01735-8

Large Forbush Decreases and their Solar Sources: Features and Characteristics

M. Papailiou[1] · M. Abunina[2] · A. Belov[2] · E. Eroshenko[2] · V. Yanke[2] · H. Mavromichalaki[1]

Received: 1 November 2019 / Accepted: 7 November 2020

Abstract One of the factors responsible for the wide variety of Forbush decreases is the different solar sources related to them. In this investigation the different features and characteristics of Forbush decreases, with emphasis on large Forbush decreases and their association with solar sources, are examined. Initially, a wider selection of events from the Pushkov Institute of Terrestrial Magnetism, Ionosphere and Radiowave Propagation of the Russian Academy of Sciences Forbush decreases database served as a starting point for this study, which was then narrowed down to a group of large Forbush decreases. According to the helio-longitude of the solar source, the events under study were separated into three subcategories: western ($21^\circ \leq$ helio-longitude $\leq 60^\circ$), eastern ($-60^\circ \leq$ helio-longitude $\leq -21^\circ$), and central ($-20^\circ \leq$ helio-longitude $\leq 20^\circ$). The selected events cover the period 1967 – 2017. The "Global Survey Method" was used for analyzing the aforementioned Forbush decreases, along with data on solar flares, solar-wind speed, geomagnetic indices (Kp and Dst), and interplanetary magnetic field. The superimposed epoch method was applied to display the temporal profiles for the selected events. This detailed analysis reveals interesting results concerning the features of cosmic-ray decreases in relation to the helio-longitude of the solar sources. Specifically, Forbush decreases related to central or eastern solar sources are more often observed, have a greater magnitude, and present a slower development than Forbush decreases related to western sources, which are rarer, have a smaller magnitude, and have a shorter lifespan. Nevertheless, regardless of the helio-longitude of the solar source, large Forbush decreases are accompanied by increased geomagnetic activity and increased anisotropy, including anisotropy before the events, which can serve as a typical precursor of Forbush decreases.

Keywords Space weather · Cosmic rays · Forbush decreases · Solar sources

✉ H. Mavromichalaki
emavromi@phys.uoa.gr

[1] Nuclear and Particle Physics Department, Faculty of Physics, National and Kapodistrian University of Athens, 15784 Athens, Greece

[2] Pushkov Institute of Terrestrial Magnetism, Ionosphere and Radiowave Propagation Russian Academy of Sciences (IZMIRAN), Troitsk, Moscow, 108840, Russia

Published online: 24 November 2020

1. Introduction

Solar-terrestrial relations define space weather, which is of great practical importance (Kudela et al., 2000; Singer, Heckman, and Hirman, 2001; Schwenn, 2006; Pulkkinen, 2007; Gopalswamy, 2009; Mavromichalaki, 2012), and this is the reason for its intense study. An aspect of this study is galactic cosmic rays interacting with the interplanetary disturbances, even before they arrive at the Earth, and therefore they provide information about the imminent disturbance before it reaches the Earth (Belov et al., 1995; Munakata et al., 2006). Specifically, solar phenomena such as coronal holes, solar flares, and coronal mass ejections define space weather (Baker, 2004; Singh, Siingh, and Singh, 2010; Gopalswamy, 2018; Archontis and Vlahos, 2019) by giving rise to solar-wind disturbances, which in turn create disturbances in the magnetosphere that can cause storms in the geomagnetic field (Kudela and Storini, 2006; Kuwabara et al., 2006). The storms are often accompanied by decreases in the cosmic-ray intensity, known as Forbush decreases (FDs), which are indicators of disturbances in the heliosphere (Forbush, 1958; Lockwood, 1971; Cane, 2000).

Consequently, a FD is not only a storm observed in the cosmic-ray intensity, but also a manifestation of a heliospheric storm (Belov, 2008). Therefore, the Forbush decrease effect can be defined as "the result of the effect of coronal mass ejections (CMEs and ICMEs) and/or high speed solar-wind streams originating from coronal holes on cosmic rays" (Papaioannou et al., 2010; Belov et al., 2014; Kryakunova et al., 2015). Forbush decreases are observed as a short-term and steep decrease of the galactic cosmic-ray intensity that is followed by a relatively slow recovery (e.g. Melkumyan et al., 2018) lasting up to one week (Forbush, 1958; Lockwood, 1971; Cane, 2000; Usoskin et al., 2008; Melkumyan et al., 2019).

It can be argued that not only the variety of solar sources, and the way in which they are combined, but also the different interplanetary conditions before and during the event and the nature of observations (Belov, 2008) are responsible for the different features of FDs. For example, FDs may vary in relation to the magnitude and the duration of the event, the fast or gradual decrease, the complete recovery or absence of recovery phase, the completion in one or two steps, the simple or complicated time profile, etc.

This study focuses on the solar sources related to a number of FDs, and it investigates their location as a factor that could provide interesting results regarding the wide variety of these events and the various manifestations of their characteristics. In particular, this study focuses on the influence of solar sources' position on the FD magnitude (i.e. on the variation of the cosmic-ray density) and on the maximum anisotropy of cosmic rays.

2. Data and Method

The Forbush-effects and interplanetary-disturbances database (FEID) of the Pushkov Institute of Terrestrial Magnetism, Ionosphere and Radiowave Propagation of the Russian Academy of Sciences (IZMIRAN) (spaceweather.izmiran.ru/eng/dbs.html) has been used for this study (Abunin et al., 2013). This database includes all of the FDs from the beginning of the neutron-monitor operation until today, as they were recorded by the global Neutron Monitor Network, which counts at least 50 stations distributed all over the Earth (Belov et al., 2015). The total number of events is ≈ 7000 over the time period 1957 – 2017 (Belov et al., 2018). Moreover, using the global survey method (GSM), the cosmic-ray density (in other words, zero spherical harmonic or isotropic part of cosmic-ray flux) in percentage and cosmic-ray anisotropy (first spherical harmonic) in percentage for the cosmic rays of rigidity 10 GV have been calculated (Belov et al., 2018) and entered into this database. It defines FD global characteristics independent of individual detectors (Abunina et al., 2013a). The above-mentioned anisotropy refers to the hourly equatorial component $[A_{xy}]$ of cosmic-ray anisotropy, i.e. the diurnal anisotropy $[=\sqrt{A_x^2 + A_y^2}]$ derived from the A_x- and A_y-components of the cosmic-ray anisotropy vector. Also, the north–south component of the anisotropy $[A_z]$ is mentioned.

In addition to solar-wind parameters (solar-wind speed and interplanetary magnetic-field IMF intensity) and geomagnetic indices (Ap, Kp, and Dst) that were obtained from the OMNI database (omniweb.gsfc.nasa.gov), the list of sudden storm commencements (SSCs) (isgi.unistra.fr/data_download.php), and data on solar flares (class, location, time) (ftp.swpc.noaa.gov/pub/indices/events/) were also used (Belov et al., 2014).

This analysis refers to Forbush decreases that began with an SSC for the time period 1967 – 2017, which are characterized by large amplitude and occurred on a relatively quiet background. This means that 48 hours before and 18 hours after the registration of the SSC, no other FDs were recorded.

3. Analysis and Results

The FEID provides the possibility of grouping Forbush decreases with respect to different criteria, which refer to solar, interplanetary, and geomagnetic parameters and various statistical estimations (Abunin et al., 2012; Abunina et al., 2013a). The FDs catalog (text files with data of various parameters of individual FDs) can be downloaded and processed by whomever is interested by using the related link on the FEID website (spaceweather.izmiran.ru/eng/dbs.html). For online sorting and selecting FDs, according to various parameters, registration is required.

In this study, the selection of events and their grouping was made using the combination of several criteria: The criterion for group A is the SSC, for group B, apart from the SSC, the magnitude is also considered, whereas the FDs of group C are being investigated with respect to SSC, magnitude, quiet background, and presence of an identified solar source. Moreover, the FDs of group C were further divided into three subcategories, according to the helio-longitude of the solar source. The resulting categories are shown in Table 1. In this table, group C includes 100 events associated with sources with helio-longitude −90° to 90°, but since FDs associated with sources from the far-eastern (−90° to −61°) and far-western (61° to 90°) regions are not being considered in the particular study, the remaining 87 FDs are organized in groups C-W, C-E, and C-C. A more detailed description of the categories of events under study is presented in the following.

Events with SSC have been selected, as the shock-wave recording time indicates the exact beginning of the FDs. The start time of Forbush effects without a shock is indicated approximately and can vary by several hours. This introduces uncertainty in the values of some characteristics of the FDs (for example, the times of extrema and the values of the parameters before the start of the FD). All other FDs also deserve consideration, but the focus of this work is FDs with a definite onset time.

In the following, three examples of FDs that evolve in a quiet background and are related to sources with different helio-longitude are analyzed. There are three panels in Figure 1: In the upper panel, the behavior of solar-wind speed (right scale, yellow curve) and IMF intensity (left scale, brown curve) are presented. The middle panel shows the cosmic-ray density (left scale, red curve) and equatorial anisotropy (right scale, blue columns) changes. The

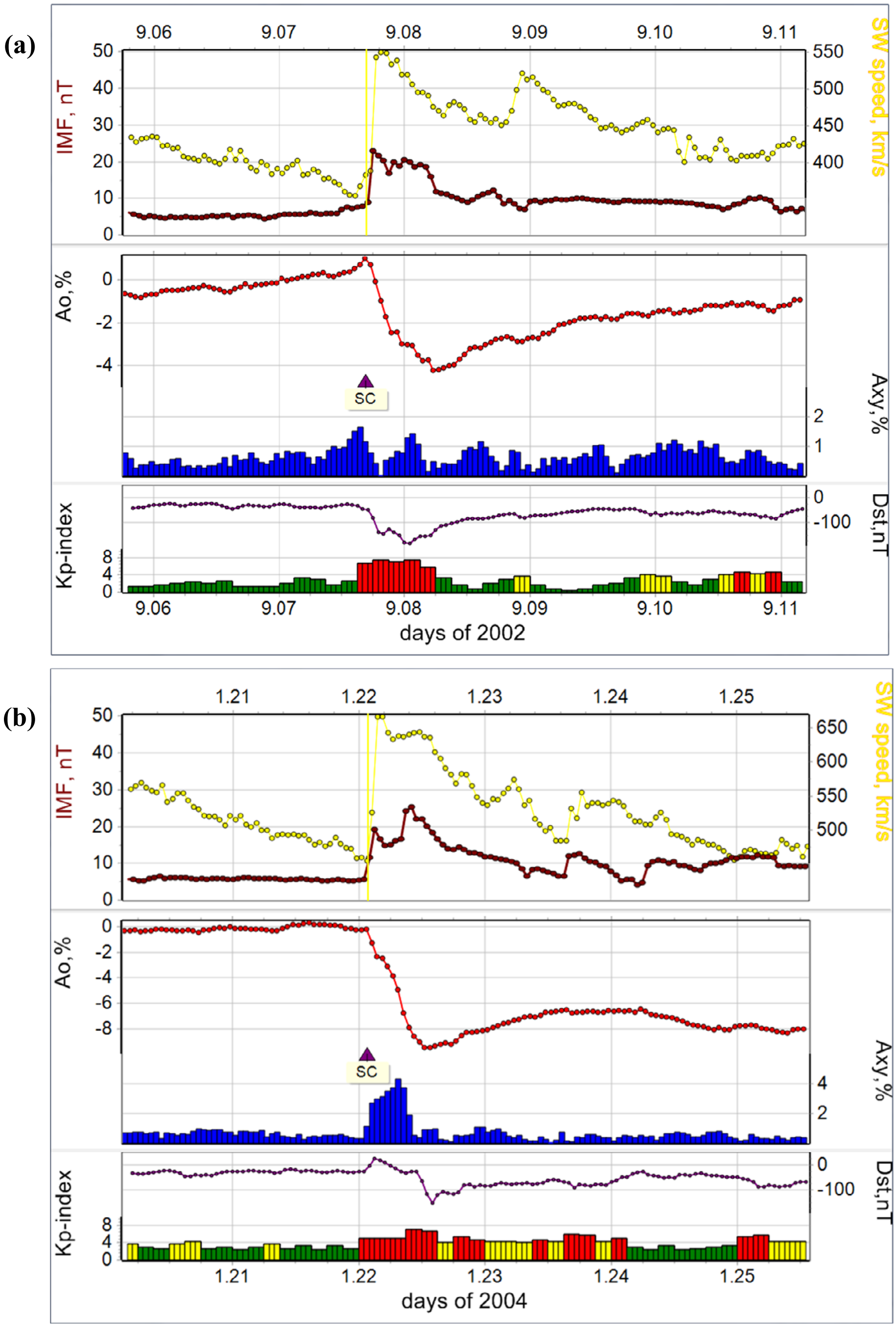

Figure 1 Variations of the interplanetary magnetic field and the solar-wind speed, the cosmic-ray density A_0, and the magnitude of the component A_{xy} of the first harmonic of anisotropy and the Dst and Kp indices for the events on (**a**) 07 September 2002, (**b**) 22 January 2004, and (**c**) 17 August 2001.

(c)

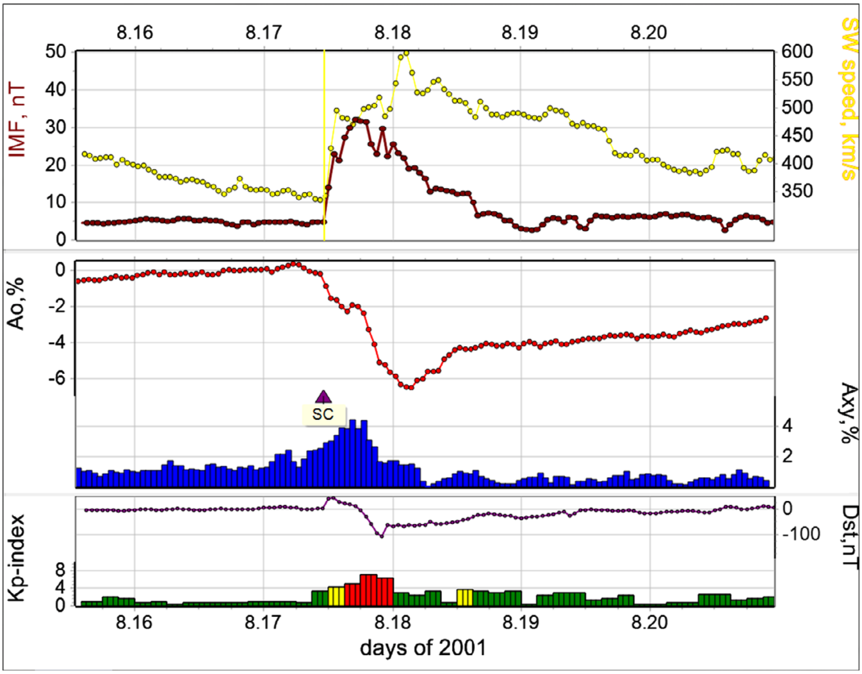

Figure 1 (*Continued.*)

behaviors of the main geomagnetic indices (left scale – Kp index, right scale – Dst index) are presented in the bottom panel. In Figure 1a the FD recorded on 07 September 2002 with an SSC registered at 16:36 UT is presented. This event has an amplitude $A_F = 5.3\%$ and maximum equatorial anisotropy $A_{xy\,\max} = 1.64\%$. The solar source of this event is a halo CME (daw.gsfc.nasa.gov/CME_list/) recorded on 05 September 2002 at 16:54 UT (with a maximal speed of 1748 $\mathrm{km\,s^{-1}}$) and associated with a solar flare of class C5.2 (registered on 05 September 2002 at 16:18 UT) with coordinates N09E28 (eastern solar source). The solar-wind speed and interplanetary magnetic field intensity are $V_{\max} = 550\ \mathrm{km\,s^{-1}}$ and $B_{\max} = 22.9$ nT, respectively. The main geomagnetic activity parameters for this FD are $\mathrm{Kp}_{\max} = 7+$ and $\mathrm{Dst}_{\min} = -101$ nT.

The FD on 22 January 2004 (Figure 1b) has an amplitude $A_F = 9\%$ and maximum anisotropy $A_{xy\,\max} = 4.32\%$. The SSC related to this event was registered at 01:37 UT. A halo CME on 20 January 2004 at 00:06 UT (with maximal speed 965 $\mathrm{km\,s^{-1}}$) associated with a class C5.5 solar flare recorded on 19 January 2004 at 22:02 UT and located at S13W09 (central solar source) is the source of this event. Moreover, the main solar-wind parameters (solar-wind speed and IMF) near the Earth are $V_{\max} = 666\ \mathrm{km\,s^{-1}}$ and $B_{\max} = 25.2$ nT, respectively, while the main geomagnetic activity parameters are $\mathrm{Kp}_{\max} = 7$ and $\mathrm{Dst}_{\min} = -149$ nT.

The FD recorded on 17 August 2001 (SSC was recorded at 11:03 UT) is an event connected to a western solar source (Figure 1c), i.e. a halo CME on 14 August 2001 at 16:01 UT (with maximal speed 618 $\mathrm{km\,s^{-1}}$), which is associated with a solar flare of class C2.3 recorded on 14 August 2001 at 11:30 UT and coordinates N16W36. The values of the main cosmic-ray parameters for this event are $A_F = 7.1\%$ and $A_{xy\,\max} = 4.41\%$. The maximum values of the solar-wind speed and the IMF are $V_{\max} = 599\ \mathrm{km\,s^{-1}}$ and $B_{\max} = 31.2$ nT,

Table 1 The criteria used in this study for grouping the Forbush decreases registered from 1967 – 2017.

Categorization	Criteria	Number of events
Group A	FDs with SSC	1515
Group B	FDs with SSC and magnitude greater than 4%	335
Group C	FDs with SSC, magnitude greater than 4%, which evolved on a quiet background (no other events were registered for 48 hours before and 18 hours after the onset of each FD) and connected to identified solar sources:	100
Group C-W	western sources ($21° \leq$ helio-longitude $\leq 60°$)	23
Group C-E	eastern sources ($-60° \leq$ helio-longitude $\leq -21°$)	28
Group C-C	central sources ($-20° \leq$ helio-longitude $\leq 20°$)	36

respectively, and the values of the geomagnetic activity parameters are $\mathrm{Kp_{max}} = 7$ and $\mathrm{Dst_{min}} = -105$ nT.

3.1. Temporal Profiles of FD Groups

For this study, firstly, a wide selection of events that present an SSC and refer to the time period 1967 – 2017 was made (Table 1). A total of 1515 FDs was identified (group A). Secondly, group A was narrowed down by selecting the magnitude of FDs greater than 4% and connected to SSC. In this way large FDs were singled out. As a result, 335 FDs were selected (group B).

From the group of 335 large FDs with SSC, large decreases, which evolved in a relatively quiet background (no other events were registered for 48 hours before and 18 hours after each FD) and connected to identified solar sources, were chosen. A total of 100 events for time period 1967 – 2017 were selected (group C) and classified according to the heliographic longitude of the solar source into three categories: i) western sources ($21° \leq$ helio-longitude $\leq 60°$) (group C-W), ii) eastern sources ($-60° \leq$ helio-longitude $\leq -21°$) (group C-E), and iii) central sources ($-20° \leq$ helio-longitude $\leq 20°$) (group C-C).

Finally, averaged temporal profiles for some parameters concerning these groups of events were plotted. Specifically, the cosmic-ray density [A_0] and the magnitude of the component [A_{xy}] of the first harmonic of anisotropy along with the interplanetary magnetic-field intensity and the solar-wind speed and the geomagnetic indices Dst and Kp for the groups C-W (Figure 2a), C-E (Figure 2b), and C-C (Figure 2c) are presented as result of the application of the superimposed-epoch method. These profiles cover a period of 48 hours before and 120 hours after the SSC.

In Figure 2a, the detail of the changes in density 44 – 30 hours before the onset of the events is not associated with modulation effects, but it is a consequence of ground-level enhancements (GLEs), which quite often precede large FDs from western solar sources. Four of the selected events are related to GLEs (13 October 1981, 26 October 1989, 04 November 2003, 14 December 2006).

The results from the superimposed-epoch method are organized in Table 2. The parameters that are most interesting are the FD magnitude [A_{F}: %], the maximum value of the equatorial component of the first harmonic of CR anisotropy [$A_{xy\,\mathrm{max}}$: %], the anisotropy one hour before the onset [A_{xyb}: %], the minimum value for the geomagnetic index Dst [$\mathrm{Dst_{min}}$], the maximum value of the interplanetary magnetic field intensity [B_{max}], and the maximum value of the solar-wind speed [V_{max}] averaged by the superimposed-epoch method

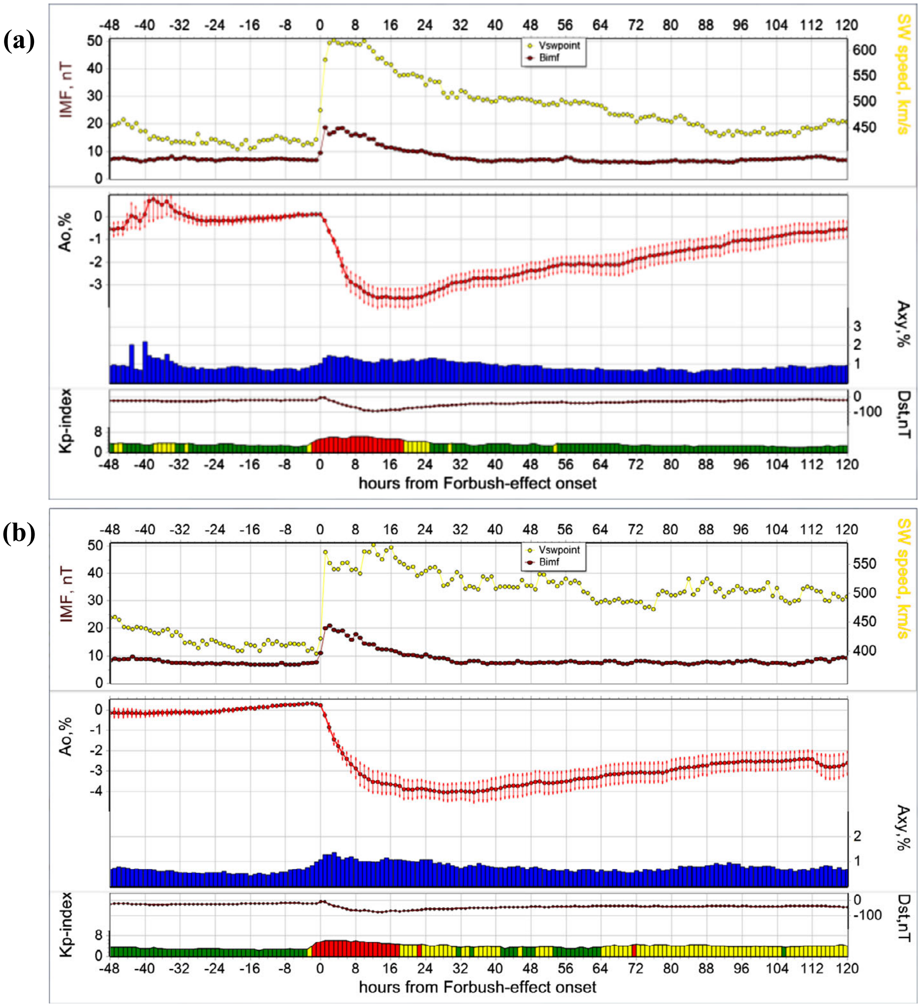

Figure 2 Variations of the interplanetary magnetic field and the solar-wind speed, the cosmic-ray density [A_0] – the magnitude of the component [A_{xy}] of the first harmonic of anisotropy, and the Dst and Kp indices for the time periods before and after the arrival of the SSC, as they were calculated by the superimposed epoch method for (**a**) 23 Forbush decreases connected to western sources, (**b**) 28 Forbush decreases connected to eastern sources, and (**c**) 36 Forbush decreases connected to central sources with magnitude $\geq 4\%$ and SSC. Zero suggests the recording time of the SSC.

for all events, and, finally, the variation during the last hour before the onset of each event [$\Delta B = B_0 - B_b$ and $\Delta V = V_0 - V_b$] where B_0 and V_0 are the interplanetary magnetic-field intensity and solar-wind speed values at the hour of the SSC recording and B_b and V_b are the interplanetary magnetic-field intensity and solar-wind speed values one hour before the onset of the event.

The groups of eastern, central, and western solar sources include 28, 36, and 23 FDs, respectively. Disturbances connected to the western limb of the Sun can be associated with space-weather effects (Lugaz, Roussev, and Sokolov, 2008). Nevertheless, in this study large FDs are most often created by central or eastern solar sources, and less often by western. The

(c)

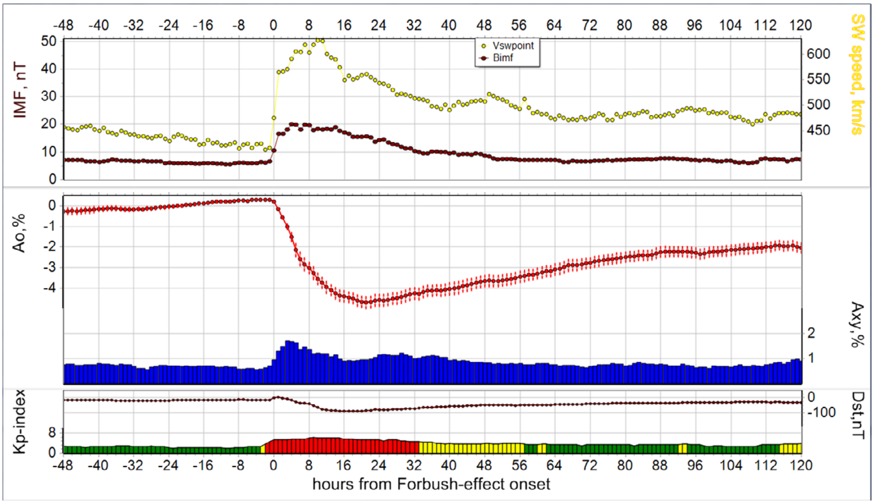

Figure 2 (*Continued.*)

Table 2 Results from the superimposed epoch method for the categories of events under study.

	1515 FDs SSC	335 FDs SSC, ampl. ≥ 4%	87 FDs SSC, ampl. ≥ 4%, quiet background, identified solar source (−60° ≤ helio-long. ≤ 60°)		
			Western sources	Eastern sources	Central sources
A_F [%]	1.75 ± 0.06	4.57 ± 0.15	3.7 ± 0.45	4.37 ± 0.52	5.01 ± 0.31
$A_{xy\,\max}$ [%]	0.96 ± 0.02	1.48 ± 0.05	1.47 ± 0.19	1.36 ± 0.18	1.70 ± 0.15
A_{xyb} [%]	0.76 ± 0.01	0.93 ± 0.04	0.94 ± 0.14	0.96 ± 0.09	0.70 ± 0.06
$\mathrm{Dst}_{\min}$ [nT]	−44.2 ± 1.3	−84.6 ± 4.17	−92.4 ± 15.46	−74.6 ± 12.38	−90.4 ± 12.1
$B_{\max}$ [nT]	13.24 ± 0.22	19.28 ± 0.63	18.66 ± 1.70	20.88 ± 2.43	20.04 ± 2.11
ΔB [nT]	2.31 ± 0.20	3.92 ± 0.48	2.71 ± 1.10	3.35 ± 1.17	4.09 ± 0.97
$V_{\max}$ [km s^{-1}]	492.8 ± 4.0	603.9 ± 10.6	619.7 ± 42.1	583.9 ± 27.3	627.0 ± 24.5
ΔV [km s^{-1}]	25.9 ± 4.4	42.5 ± 11.5	56.7 ± 35.6	25.8 ± 19.2	59.3 ± 22.7

magnitude of the events connected to western solar sources (3.7%) is obviously smaller than that of the events connected to eastern (4.37%) or central sources (5.01%) (Abunina et al., 2013a). The typical value for the parameter of anisotropy during quite conditions is 0.53% (Abunina et al., 2013b; Belov et al., 2017). Moreover, the usual value of anisotropy one hour before the FD is ≈ 0.7% (Belov et al., 2008), which agrees with the result for FDs with SSC (0.76%) and the FDs related to central sources (0.70%). However, for the large FDs there is an observed increase of the A_{xyb} almost up to 1%. As seen in Table 2, the anisotropy one hour before the onset of the FD is almost the same (0.94 and 0.96), regardless of the location of the solar source (western or eastern) and its value significantly exceeds the typical value of anisotropy during quiet conditions (Abunina et al., 2013b). This, apparently, is a consequence of an increase of the CR density gradient in this part of the solar-wind disturbance. This confirms the assumption that increased vector anisotropy is one of the typical precursors of FDs (Belov et al., 2008; Papailiou et al., 2012). Interplanetary conditions (solar-wind

Table 3 Average values of different parameters concerning the 1515 FDs with SSC, the 335 large FDs ($A_F \geq 4\%$) with SSC and the 87 large FDs ($A_F \geq 4\%$), with SSC, which evolved in a quiet background and had identified solar sources ($-60^\circ \leq$ helio-long. $\leq 60^\circ$).

Parameter	1515 FDs SSC	335 FDs SSC, $A_F \geq 4\%$	87 FDs SSC, $A_F \geq 4\%$, quiet background, identified solar source ($-60^\circ \leq$ helio-long.60°)
A_F [%]	2.63 ± 0.07	6.15 ± 0.19	5.91 ± 0.34
$A_{xy\,\mathrm{max}}$ [%]	1.75 ± 0.02	2.67 ± 0.06	2.53 ± 0.10
Az_{range} [%]	2.12 ± 0.03	3.12 ± 0.07	2.98 ± 0.11
$A_{xy\mathrm{b}}$ [%]	0.934 ± 0.017	1.352 ± 0.050	1.296 ± 0.083
D_{min} [%]	-0.61 ± 0.02	-1.29 ± 0.05	-1.12 ± 0.09
$\mathrm{Kp}_{\mathrm{max}}$	5.42 ± 0.04	6.88 ± 0.07	6.66 ± 0.15
$\mathrm{Ap}_{\mathrm{max}}$ [2 nT]	79.0 ± 1.8	149.7 ± 5.1	133.7 ± 8.3
$\mathrm{Dst}_{\mathrm{min}}$ [nT]	-70.3 ± 1.6	-129.7 ± 4.9	-120.8 ± 8.6
B_{max} [nT]	17.15 ± 0.25	24.79 ± 0.68	25.13 ± 1.18
V_{max} [km s^{-1}]	553.9 ± 4.3	657.0 ± 10.1	646.6 ± 16.2
$V_{\mathrm{m}}B_{\mathrm{m}}$	4.97 ± 0.11	8.37 ± 0.34	8.43 ± 0.61
t_{min} [hour]	15.08 ± 0.36	18.30 ± 0.65	20.57 ± 1.14
$T[D_{\mathrm{min}}]$ [hour]	9.40 ± 0.30	7.02 ± 0.43	5.59 ± 0.71
A_F/B_{max}	0.156 ± 0.004	0.274 ± 0.010	0.261 ± 0.014
HLon	-1.083 ± 1.653	-5.565 ± 2.804	-3.172 ± 3.269

speed and IMF) are considerably increased for the large FDs in comparison to all the FDs with an SSC, as is shown in Table 2. Nevertheless, regarding the helio-longitude, FDs related to central sources seem to evolve in more disturbed interplanetary conditions, and FDs related to eastern sources have minimal averaged V_{max}.

3.2. FDs and Solar Sources

Average values of different parameters connected to the Forbush decreases under investigation are shown in Tables 3 and 4. More specifically, the parameters that are being presented are the averaged of FD maximum value [A_F], the maximum value of the equatorial component of the first harmonic of CR anisotropy [$A_{xy\,\mathrm{max}}$], the range of variations in the anisotropy north–south component [Az_{range}], the value of the equatorial component of the first harmonic of CR anisotropy one hour before the SSC [$A_{xy\mathrm{b}}$], the maximum decrease in the CR density per hour [D_{min}], the maximum and minimum values of the geomagnetic activity indices during the considered events [$\mathrm{Kp}_{\mathrm{max}}$, $\mathrm{Ap}_{\mathrm{max}}$, and $\mathrm{Dst}_{\mathrm{min}}$], the maximum IMF intensity [B_{max}], the maximum solar-wind speed [V_{max}], and the product of the maximum characteristics of the interplanetary medium in the considered disturbance calculated from the formula [$V_{\mathrm{m}}B_{\mathrm{m}} = \frac{V_{\mathrm{max}}}{V_{\mathrm{q}}}\frac{B_{\mathrm{max}}}{B_{\mathrm{q}}}$, where V_{q} and B_{q} are the parameters of a quiet medium ($V_{\mathrm{q}} = 400$ km s^{-1} and $B_{\mathrm{q}} = 5$ nT are used as a rule)], the time from the onset to the density minimum in a FD [t_{min}], the time of the maximum hourly density decrease during the main FD phase [$t(D_{\mathrm{min}})$], the ratio of the FD magnitude to the maximum IMF intensity [A_F/B_{max}], and the source helio-longitude [HLon].

As shown in Table 3, for large FDs ($A_F \geq 4\%$) there is a notable enhancement in the maximum value of the equatorial component of the first harmonic of CR anisotropy $A_{xy\,\mathrm{max}}$ (2.67% and 2.53% for the two groups of 335 FDs and 87 FDs, respectively). Furthermore, the value of the equatorial component of the first harmonic of CR anisotropy one hour before the SSC [A_{xyb}] is also increased, which highlights the fact that increased anisotropy can indicate the upcoming FDs (Leerungnavarat, Ruffolo, and Bieber, 2003; Kuwabara et al., 2004; Munakata et al., 2005; Belov et al., 2008; Papailiou et al., 2012). Moreover, the FDs of group B (335 large FDs) are accompanied by strong geomagnetic activity, i.e. $\mathrm{Dst_{min}} = -129.7$ nT, $\mathrm{Kp_{max}} = 6.88$, and $\mathrm{Ap_{max}} = 149.7$, and evolved in a somewhat more disturbed interplanetary medium ($V_{\mathrm{max}} = 657.0\ \mathrm{km\,s^{-1}}$) in comparison to the FDs of group C (87 large FDs). A significant difference is observed for the parameters D_{min} and $t(D_{\mathrm{min}})$. For the group with the 1515 events, the maximum decrease in the CR density per hour [D_{min}] is significantly less than that of the other groups and is observed several hours later.

Central and eastern sources not only provide more FDs, but also the FDs related to those sources are significantly larger in magnitude in comparison to western sources (Belov, 2008). However, FDs related to western sources are characterized by higher values of A_{xyb} (Papailiou et al., 2013). On the other hand, the maximum anisotropy for central sources is the highest (Table 4), but there is a noteworthy difference between $A_{xy\,\mathrm{max}}$ for western (2.58%) and eastern (2.22%) sources. FDs connected to central sources evolved in a more disturbed interplanetary medium (the highest values for solar-wind speed and IMF intensity are 660.2 $\mathrm{km\,s^{-1}}$ and 27.07 nT, respectively) and are accompanied by strong geomagnetic activity, i.e. $\mathrm{Dst_{min}} = -135.9$ nT, $\mathrm{Kp_{max}} = 6.8$, and $\mathrm{Ap_{max}} = 139.9$. Geomagnetic activity is more pronounced for FDs related to western sources ($\mathrm{Dst_{min}} = -115.7$ nT, $\mathrm{Kp_{max}} = 6.75$, and $\mathrm{Ap_{max}} = 138.6$) rather than those connected to eastern sources ($\mathrm{Dst_{min}} = -105.7$ nT, $\mathrm{Kp_{max}} = 6.42$, and $\mathrm{Ap_{max}} = 121.6$), although the difference is not so big. Moreover, FDs connected to western sources reach the minimum more rapidly ($t_{\mathrm{min}} = 18.35$ hours) than those related to eastern or central sources, which develop more slowly ($t_{\mathrm{min}} = 22.61$ hours and $t_{\mathrm{min}} = 20.42$ hours) (Abunina et al., 2013a).

The western-sources category includes FDs with magnitude that varies from 4% (FD on 4 November 2003) to 13.5% (FD on 26 July 2004), while the anisotropy value is over 4% for three events (9 September 1992, 17 August 2001, and 14 December 2006). Strong or in some cases severe geomagnetic activity accompanies the majority of events; the Kp index has values > 6 and maximum value 8.7 (FD on 26 July 2004), while the Dst index values are also low. For example, for nine FDs of this group (5 March 1981, 10 October 1988, 17 November 1989, 30 March 1990, 9 September 1992, 24 November 2001, 26 July 2004, 14 December 2006, and 17 March 2015) Dst index is −215 nT, −156 nT, −266 nT, −187 nT, −135 nT, −221 nT, −197 nT, −146 nT and −223 nT, respectively. Moreover, increased values were observed not only for the IMF (maximum value of 56.9 nT for the FD on 24 November 2001) but also for the solar-wind speed, which was over 1000 $\mathrm{km\,s^{-1}}$ in two cases, during the FD on 26 July 2004 (1027 $\mathrm{km\,s^{-1}}$) and the FD on 24 November 2001 (1040 $\mathrm{km\,s^{-1}}$).

The eastern-sources category included FDs with Kp index value ranging from 4 to 9 (FD on 13 July 1982), while values for the Dst index vary from considerably high (−11 nT during the FD on 13 July 1978) to extremely low, for example −218 nT, −211 nT, and −325 nT during FDs on 1 April 1976, 1 March 1982, and 13 July 1982, respectively. During the event on 13 July 1982, the maximum magnitude (22.8%), anisotropy (4.71%), and solar-wind speed (986 $\mathrm{km\,s^{-1}}$) in relation to the rest of the events of this category have been recorded. Maximum IMF intensity (54.4 nT) was recorded during the event on 6 June 1979.

Interplanetary magnetic-field intensity and solar-wind speed for the events included in the central-sources group varied from 14.3 nT (FD on 18 August 2002) to 55.8 nT (FD on 20 November 2003) and from 456 $\mathrm{km\,s^{-1}}$ (FD on 15 February 2014) to 959 $\mathrm{km\,s^{-1}}$ (FD on 15 May 2005). The majority of the events of this particular category are connected to strong,

Table 4 Average values of different parameters concerning the large FDs related to western, eastern, and central sources.

Parameter	87 FDs SSC, $A_F \geq 4\%$, quiet background, identified solar source ($-60° \leq$ helio-long. $\leq 60°$)		
	Western sources	Eastern sources	Central sources
A_F [%]	5.16 ± 0.56	5.59 ± 0.61	6.64 ± 0.57
$A_{xy\,\max}$ [%]	2.58 ± 0.2	2.22 ± 0.14	2.73 ± 0.18
Az_{range} [%]	2.84 ± 0.24	3.14 ± 0.21	2.94 ± 0.15
A_{xyb} [%]	1.350 ± 0.143	1.296 ± 0.139	1.262 ± 0.144
$D_{\min}$ [%]	-1.07 ± 0.17	-0.98 ± 0.16	-1.25 ± 0.15
$\text{Kp}_{\max}$	6.75 ± 0.30	6.42 ± 0.25	6.8 ± 0.23
$\text{Ap}_{\max}$ [2 nT]	138.6 ± 15.9	121.6 ± 15.0	139.9 ± 13.0
$\text{Dst}_{\min}$ [nT]	-115.7 ± 15.3	-105.7 ± 13.4	-135.9 ± 14.8
$B_{\max}$ [nT]	22.56 ± 2.29	24.77 ± 2.20	27.07 ± 1.75
$V_{\max}$ [km s^{-1}]	660.5 ± 36.3	614.5 ± 26.9	660.2 ± 23.2
$V_m B_m$	7.87 ± 1.32	7.87 ± 1.03	9.25 ± 0.91
$t_{\min}$ [hour]	18.35 ± 2.28	22.61 ± 2.12	20.42 ± 1.67
$t(D_{\min})$ [hour]	6.00 ± 1.40	4.32 ± 1.26	6.31 ± 1.10
$A_F/B_{\max}$	0.272 ± 0.027	0.247 ± 0.027	0.263 ± 0.022
HLon	37.261 ± 2.471	-36.929 ± 1.752	-2.75 ± 2.003

severe, or in some cases extreme storms with Kp index maximum value being 8.7 (FDs on 8 November 1991 and 20 November 2003) and Dst index reaching low values for a significant number of events. For example, the lowest Dst index value was recorded for the events on 21 September 1982 (−210 nT), 9 January 1983 (−213 nT), 4 February 1983 (−183 nT), 20 October 1989 (−268 nT), 8 July 1991 (−194nT), 8 November 1991 (−354 nT), 20 November 2003 (−422 nT), and 15 May 2005 (−263 nT). Moreover, the magnitude for three FDs of this group exceeds 10% (23.4% for the FD on 20 October 1989, 15.2% for the FD on 27 November 1989, and 12.3% for the FD on 15 May 2005), while maximum anisotropy is above 4% for six events (4.51% for the FD on 21 September 1982, 4.25% for the FD on 4 January 1988, 5.01% for the FD on 20 October 1989, 4.45% for the FD on 27 November 1989, 4.45% for the FD on 8 July 1991, and 4.32% for the FD on 22 January 2004).

4. Summary

Forbush decreases of the cosmic-ray intensity, along with other effects of space weather, can influence a wide range of human activities from technological systems to human health (e.g. Schwenn, 2006). That being the case, the scientific community can benefit greatly by all of the studies that provide accurate and reliable information about such effects.

This study refers to a group of large Forbush decreases, i.e. FDs with magnitude $\geq 4\%$ for particles of 10 GV that evolve in a quiet background (with a time difference of 48 and 18 hours from the previous and next event, respectively), with identified solar sources, and that were accompanied by an SSC. The FDs were selected from the IZMIRAN Forbush-effects and interplanetary-disturbances database and cover the period from 1967 – 2017.

These events were grouped into three categories (C-W, C-E, and C-C) according to the helio-longitude of their solar sources.

The features of the events with different solar sources are highlighted and summarized as follows:

i) Large FDs ($\geq 4\%$) related to central or eastern sources are more often observed, whereas events from western sources are the rarest.
ii) The magnitude of the FDs connected to western solar sources seems to be somewhat smaller than that of eastern or central sources.
iii) FDs connected to western sources have a shorter life span in comparison to FDs connected to eastern or central sources, which present a slower development.
iv) The averaged anisotropy one hour before the SSC is increased for all groups.
v) The anisotropy one hour before the SSC is somewhat greater in FDs related to western sources than in those related to eastern or central sources.
vi) Increased vector anisotropy is one of the typical precursors of FDs.
vii) FDs related to central sources evolved in more disturbed interplanetary conditions, which is reflected in a larger IMF increase.
viii) In general, large FDs ($\geq 4\%$) are accompanied by moderate geomagnetic storms; however, some events are related to severe or even extreme geomagnetic conditions.

The aim of this study was to highlight the differences in Forbush-decrease parameters regarding the helio-longitude of the solar sources related to these events. However, this is only a first step in this direction and much more remains to be done. A future, detailed and analytic investigation on Forbush decreases and their solar sources would enrich the existing knowledge of these events and of the way they depend on solar disturbances, and it would eventually provide the necessary information for the development of a predictive system for space-weather phenomena.

Acknowledgments The authors would like to acknowledge the NMDB database (www.nmdb.eu), founded under the European Union's FP7 Program (contract no. 213007) for providing high-resolution cosmic-ray data. They would also like to thank all PIs and their colleagues of the neutron-monitor stations for kindly providing their data for this study. This work was partly supported by the Basic Research Program of the Presidium of the Russian Academy of Sciences No. 3 and 12, the RFBR grants 18-02-00451 and 20-02-00774. Work is based on the experimental data of the "Russian National Network of Cosmic Ray Stations" (SCR Network). This work was partly supported by the project ISEST/MiniMax24 (International Study of Earth-affecting Solar Transients) in the VarSITI. We would also acknowledge the anonymous reviewers for their useful suggestions significantly improving this work.

Conflict of interest The authors declare that there is no conflict of interest.

References

Abunin, A., Abunina, M., Belov, A., Eroshenko, E., Oleneva, V., Yanke, V.: 2012, *Geomagn. Aeron.* **52**, 292. DOI.

Abunin, A., Abunina, M., Belov, A., Eroshenko, E., Oleneva, V., Yanke, V.: 2013, *J. Phys. Conf. Ser.* **409**, 012165. DOI.

Abunina, M., Abunin, A., Belov, A., Eroshenko, E., Asipenka, A., Oleneva, V., Yanke, V.: 2013a, *Geomagn. Aeron.* **53**, 10. DOI.

Abunina, M.A., Abunin, A.A., Belov, A.V., Eroshenko, E.A., Oleneva, V.A., Yanke, V.G.: 2013b, *Geomagn. Aeron.* **53**, 561. DOI.

Archontis, V., Vlahos, L.: 2019, *Phil. Trans. Roy. Soc., Math. Phys. Eng. Sci.* **377**, 0152. DOI.

Baker, D.N.: 2004, *Introduction to Space Weather, Part I Introduction*, *Lect. Notes Phys.* **656**, 3. DOI.

Belov, A.V.: 2008, In: Gopalswamy, N., Webb, D.F. (eds.) *Universal Heliophysical Processes*, *Proc. IAU Symp.* **257**, Cambridge University Press, Cambridge, 439. DOI.

Belov, A., Dorman, L.I., Eroshenko, E., Iucci, N., Villoresi, G., Yanke, V.G.: 1995, In: Iucci, N., Lamanna, E. (eds.) *Proc. 24th ICRC* **4**, 888.

Belov, A.V., Dryn, E., Eroshenko, E.A., Kryakunova, O., Oleneva, V., Yanke, V.G., Papailiou, M.: 2008, In: Kiraly, P., Kudela, K., Stehlik, M., Wolfendale, A.W. (eds.) *Proc. 21-St ECRS*, Inst. Exp. Phys., Slovak Acad. Sciences, Kosice, 347.

Belov, A., Abunin, A., Abunina, M., Eroshenko, E., Oleneva, V., Yanke, V., Papaioannou, A., Mavromichalaki, H., Gopalswamy, N., Yashiro, S.: 2014, *Solar Phys.* **289**, 3949. DOI.

Belov, A., Abunin, A., Abunina, M., Eroshenko, E., Oleneva, V., Yanke, V., Papaioannou, A., Mavromichalaki, H.: 2015, *Solar Phys.* **290**, 1429. DOI.

Belov, A.V., Abunina, M.A., Abunin, A.A., Eroshenko, E.A., Oleneva, V.A., Yanke, V.G.: 2017, *Geomagn. Aeron.* **57**, 389. DOI.

Belov, A., Eroshenko, E., Yanke, V., Oleneva, V., Abunin, A., Abunina, M., Papaioannou, A., Mavromichalaki, H.: 2018, *Solar Phys.* **293**, 68. DOI.

Cane, H.: 2000, *Space Sci. Rev.* **93**, 55. DOI.

Forbush, S.E.: 1958, *J. Geophys. Res.* **63**, 651. DOI.

Gopalswamy, N.: 2009, In: Tsuda, T., Fujii, R., Shibata, K., Geller, M.A. (eds.) *Selected Papers 2007 Kyoto Symp.* **77**, TERRAPUB, Tokyo.

Gopalswamy, N.: 2018, *Extreme Events in Geospace: Origins, Predictability, and Consequences*, 37. DOI.

Kryakunova, O., Belov, A., Abunin, A., Abunina, M., Eroshenko, E., Malimbayev, A., Tsepakina, I., Yanke, V.: 2015, *J. Phys.* **CS-632**, 012062. DOI.

Kudela, K., Storini, M.: 2006, *Adv. Space Res.* **37**, 1443. DOI.

Kudela, K., Storini, M., Hofer, M.Y., Belov, A.: 2000, In: Bieber, J.W., Eroshenko, E., Evenson, P., Flückiger, E.O., Kallenbach, R. (eds.) *Cosmic Rays and Earth. Space Sciences Series of ISSI* **10**, Springer, Dordrecht. DOI.

Kuwabara, T., Munakata, K., Yasue, S., Kato, C., Akahane, S., Koyama, M., Bieber, J.W., Evenson, P., Pyle, R., Fujii, Z., Tokumaru, M., Kojima, M., Marubashi, K., Duldig, M.L., Humble, J.E., Silva, M.R., Trivedi, N.B., Gonzalez, W.D., Schuch, N.J.: 2004, *Geophys. Res. Lett.* **31**, L19803. DOI.

Kuwabara, T., Bieber, J.W., Clem, J., Evenson, P., Pyle, R., Munakata, K., Yasue, S., Kato, C., Akahane, S., Koyama, M., Fujii, Z., Duldig, M.L., Humble, J.E., Silva, M.R., Trivedi, N.B., Gonzalez, W.D., Schuch, N.J.: 2006, *Space Weather* **4**, S08001. DOI.

Leerungnavarat, K., Ruffolo, D., Bieber, J.W.: 2003, *Astrophys. J.* **593**, 587. DOI.

Lockwood, J.A.: 1971, *Space Sci. Rev.* **12**, 658. DOI.

Lugaz, N., Roussev, I.I., Sokolov, I.V.: 2008, In: Gopalswamy, N., Webb, D., Nindos, A. (eds.) *Universal Heliophysical Processes Proc. IAU Symp.* **257**, Cambridge University Press, Cambridge, 391. DOI.

Mavromichalaki, H.: 2012, In: Maris, G., Demetrescu, C. (eds.) *J. Atmos. Sol.-Terr. Phys.*, 135 ISBN:978-81-308-0483-5.

Melkumyan, A.A., Belov, A.V., Abunina, M.A., Abunin, A.A., Eroshenko, E.A., Oleneva, V.A., Yanke, V.G.: 2018, *Geomagn. Aeron.* **58**, 615. DOI.

Melkumyan, A.A., Belov, A.V., Abunina, M.A., Abunin, A.A., Eroshenko, E.A., Oleneva, V.A., Yanke, V.G.: 2019, *J. Solar-Terr. Phys.* **5**, 28. DOI.

Munakata, K., Kuwabara, T., Yasue, S., Kato, C., Akahane, S., Koyama, M., Ohashi, Y., Okada, A., Aoki, T., Mitsui, K., Kojima, H., Bieber, J.W.: 2005, *Geophys. Res. Lett.* **32**, L03S04. DOI.

Munakata, K., Yasue, S., Kato, C., Kota, J., Tokumaru, M., Kojima, M., Darwish, A.A., Kuwabara, T., Bieber, J.W.: 2006, *Adv. Geosci.* **2**, 115. DOI.

Papailiou, M., Mavromichalaki, H., Belov, A., Eroshenko, E., Yanke, V.: 2012, *Solar Phys.* **276**, 337. DOI.

Papailiou, M., Abunina, M., Mavromichalaki, H., Belov, A., Eroshenko, E., Yanke, V., Kryakunova, O.: 2013, *Solar Phys.* **283**, 557. DOI.

Papaioannou, A., Malandraki, O., Belov, A., Skoug, R., Mavromichalaki, H., Eroshenko, E., Abunin, A.: 2010, *Solar Phys.* **266**, 181. DOI.

Pulkkinen, T.: 2007, *Liv. Rev. Solar Phys.* **4**, 1. DOI.

Schwenn, R.: 2006, *Liv. Rev. Solar Phys.* **3**, 2. DOI.

Singer, H.J., Heckman, G.R., Hirman, J.W.: 2001 *Space Weather Geophys. Mono.* **125**, AGU, Washington. DOI.

Singh, A.K., Siingh, D., Singh, R.P.: 2010, *Surv. Geophys.* **31**, 581. DOI.

Usoskin, I.G., Braun, I., Gladysheva, O.G., Hörandel, J.R., Jämsén, T., Kovaltsov, G.A., Starodubtsev, S.A.: 2008, *J. Geophys. Res. Space Phys.* **113**, A07102. DOI.